Elastic, Plastic, Cracking Aspects of Material Behaviors in Indentation Hardness Tests

Ron Armstrong
Cavendish Laboratory
University of Cambridge
31 March 2011

Hardness Aspects of Elastic, Plastic, Cracking Behaviors

OUTLINE

1.Hardness stress-strain comparisons

2.Elastic (Hertzian) prediction/measurements

3. Plastic behaviors

3.1. Crystal dislocation observations

3.2. Polycrystal grain boundary hardnesses

3.3. Hall-Petch results

4. Cracking/indentation fracture mechanics

5. Summary

Hardness stress-strain comparisons

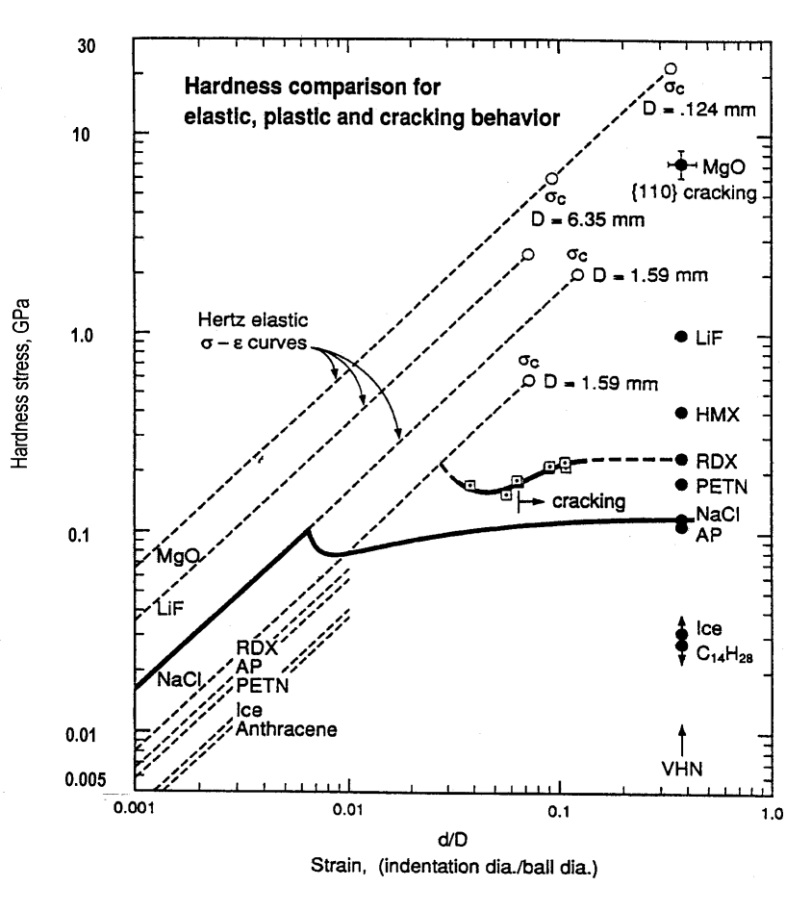

R.W. Armstrong and W.L. Elban, "Macro- to Nano-indentation Hardness Stress – Strain Aspects of Crystal Elastic/Plastic/Cracking Behaviors", *Exp. Mech.*, **50** (2010) 545-552.

Comparison of NaCl and RDX hardnesses

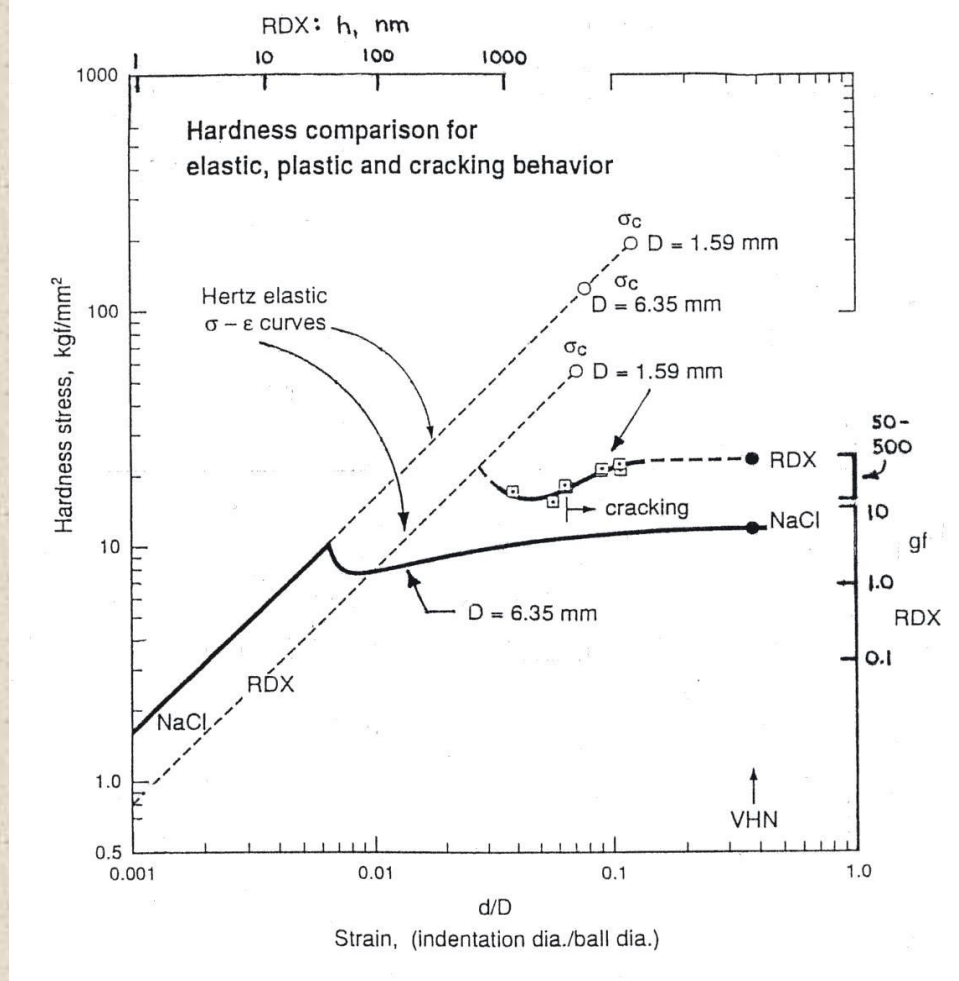

$\sigma_E = {}_{1/2}(4/3\pi)[(1 - \nu_b^2)/E_b + (1 - \nu_s^2)/E_s)]^{-1}(d/D)$ and $\sigma_c \geq [4E_s\gamma/\pi D(1 - \nu_s^2)(K_1^2 + K_2^2)]^{1/2}(d/D)^{-}$

KCl ball-type continuous load – deformation curve (D = 6.35 mm)

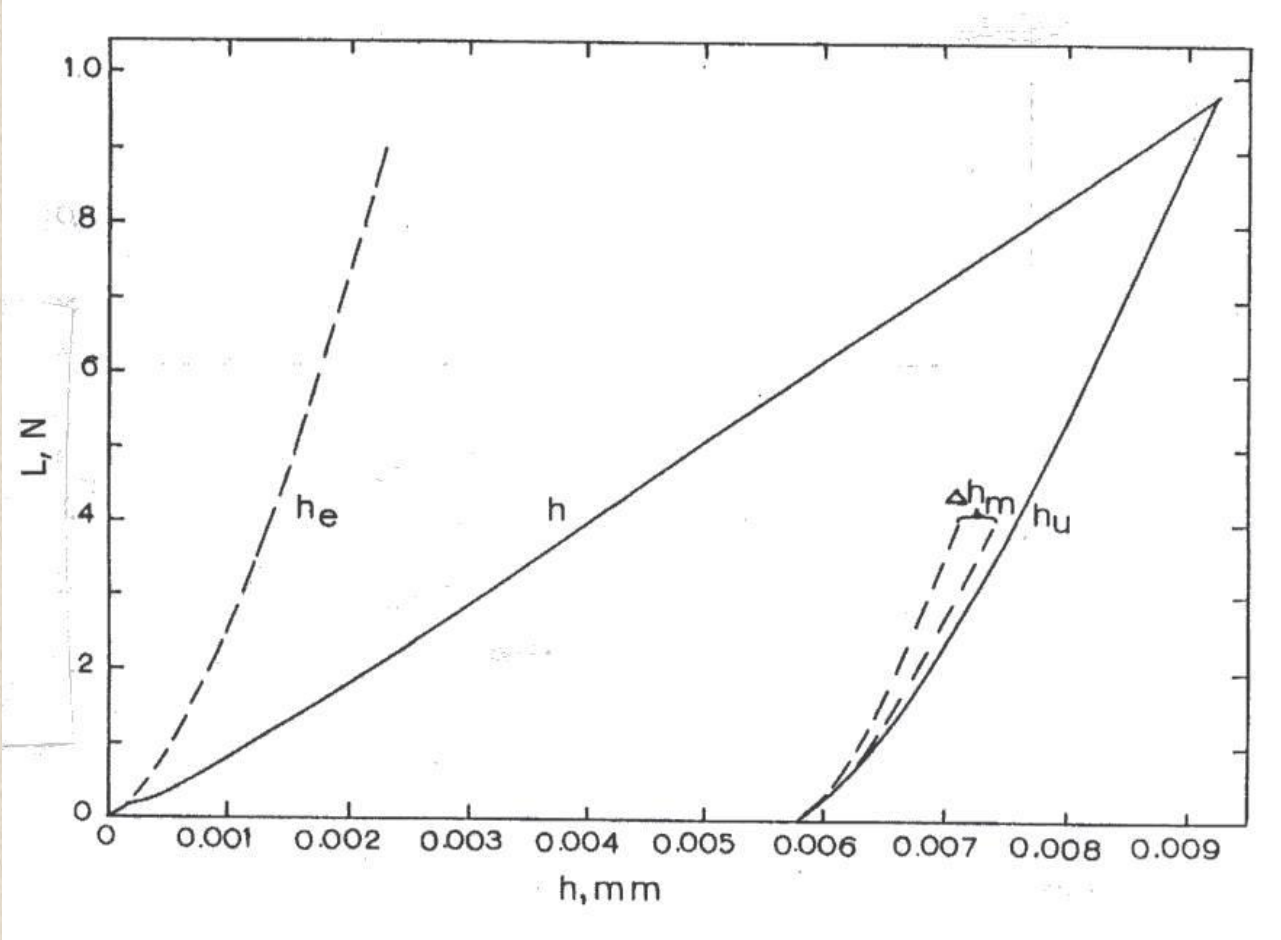

R.W. Armstrong and W.H. Robinson, *New Zealand J. Sci.*, **17**, 429-433 (1974)

NaCl result comparison with Hertzian prediction

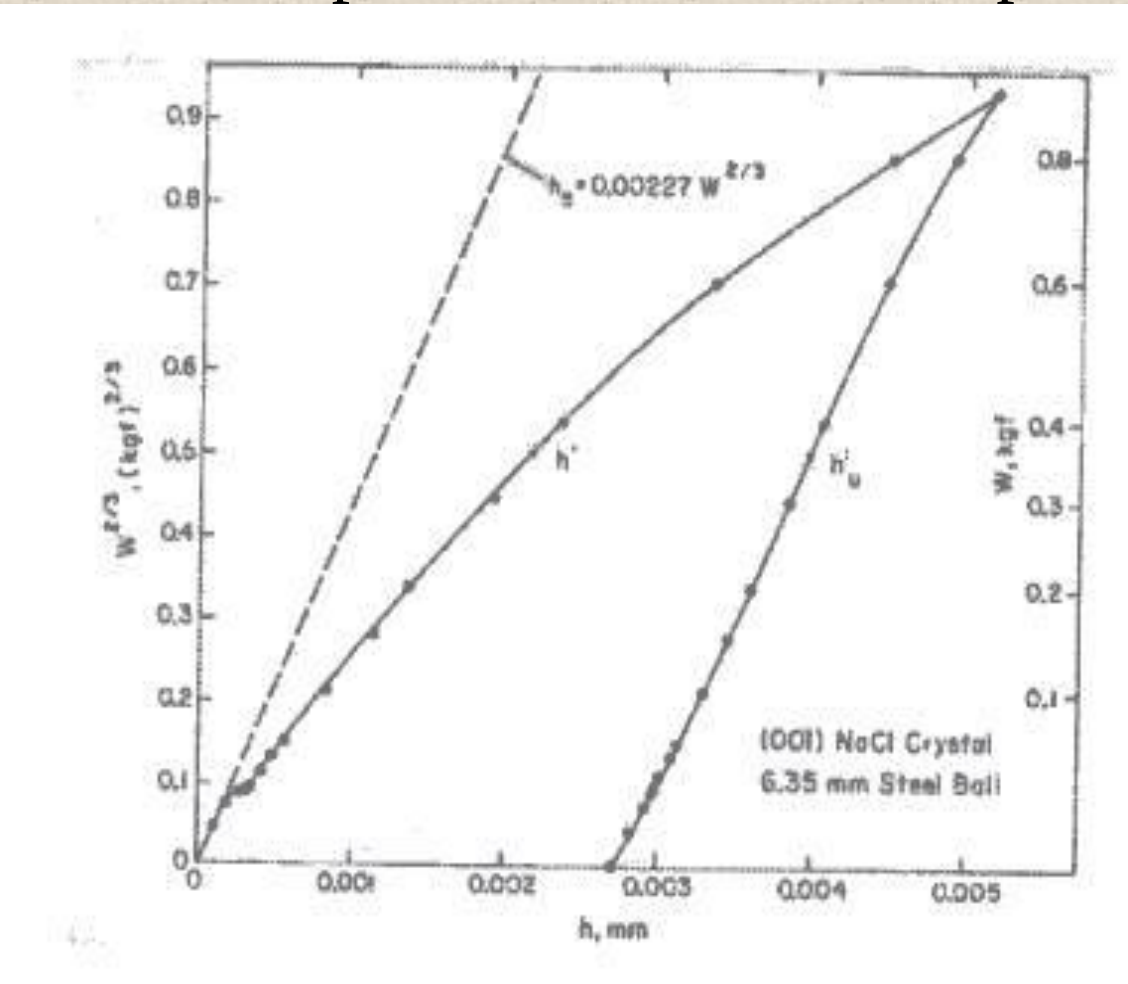

$$W^{2/3} = 2(D/9)^{1/3}[(1 - \nu_b^2)/E_b + (1 - \nu_s^2)/E_s]^{-2/3}h;\ W = P$$

Loading/unloading results for lignin

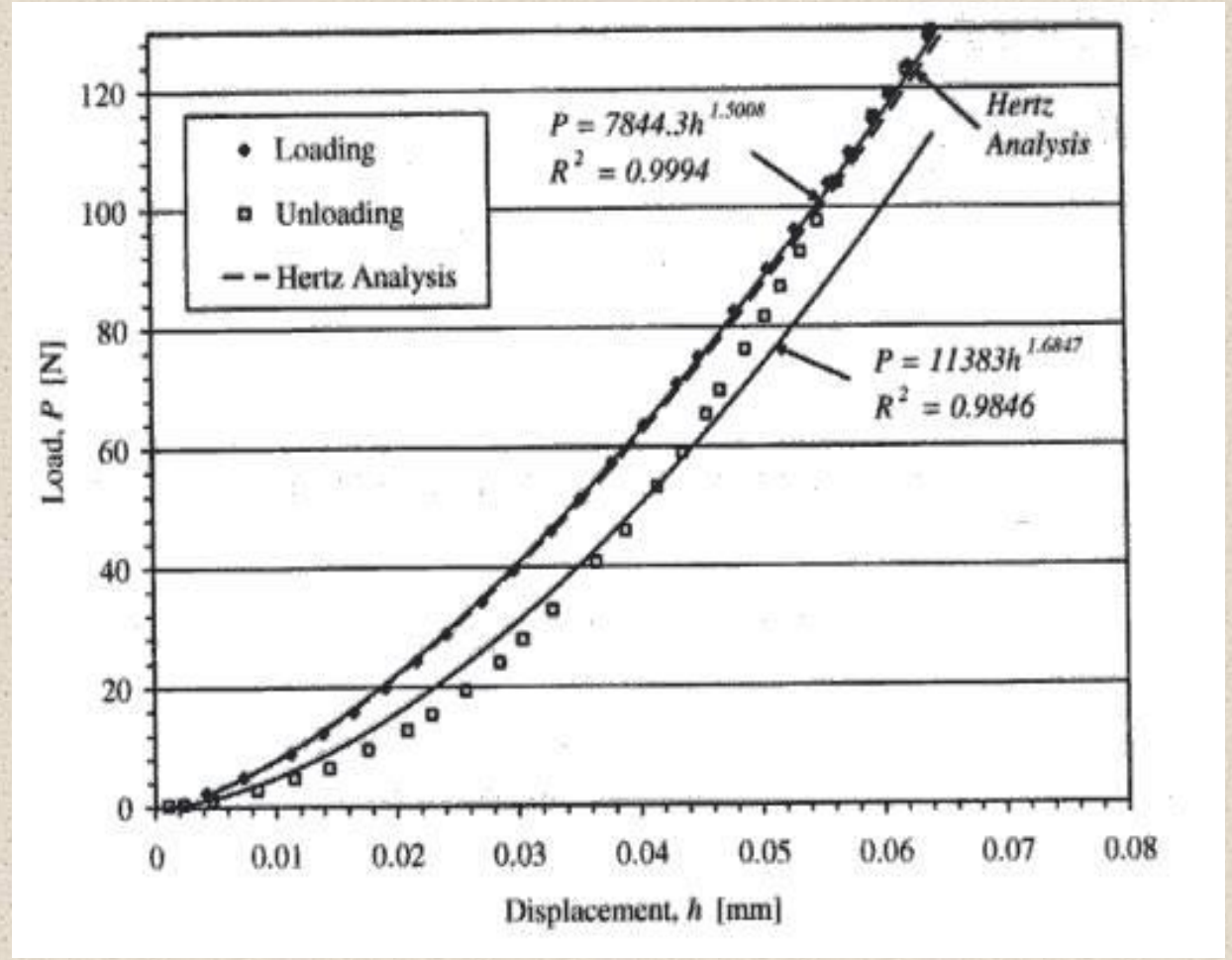

L. Ferranti, Jr., R.W. Armstrong, and N.N. Thadhani, *Mater. Sci. Eng. A*, **371**, 251-255 (2004)

Elastic modulus for 96.7% dense H2 Al

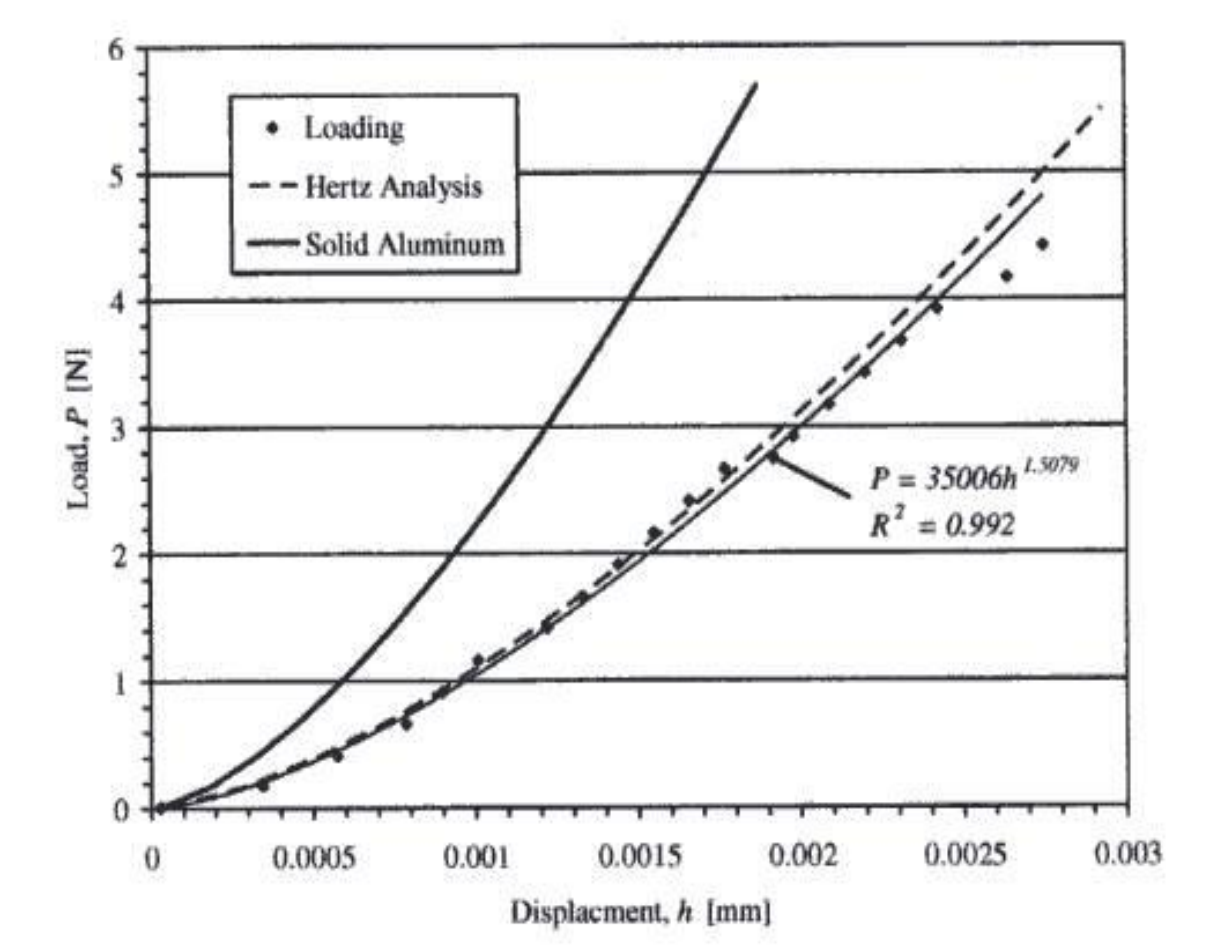

L. Ferranti, Jr., R.W. Armstrong and N.N. Thadhani, *Mater. Sci. Eng. A*, **371**, 252-255 (2004)

Elastic/plastic loading curve for 96.7% dense H2 Al

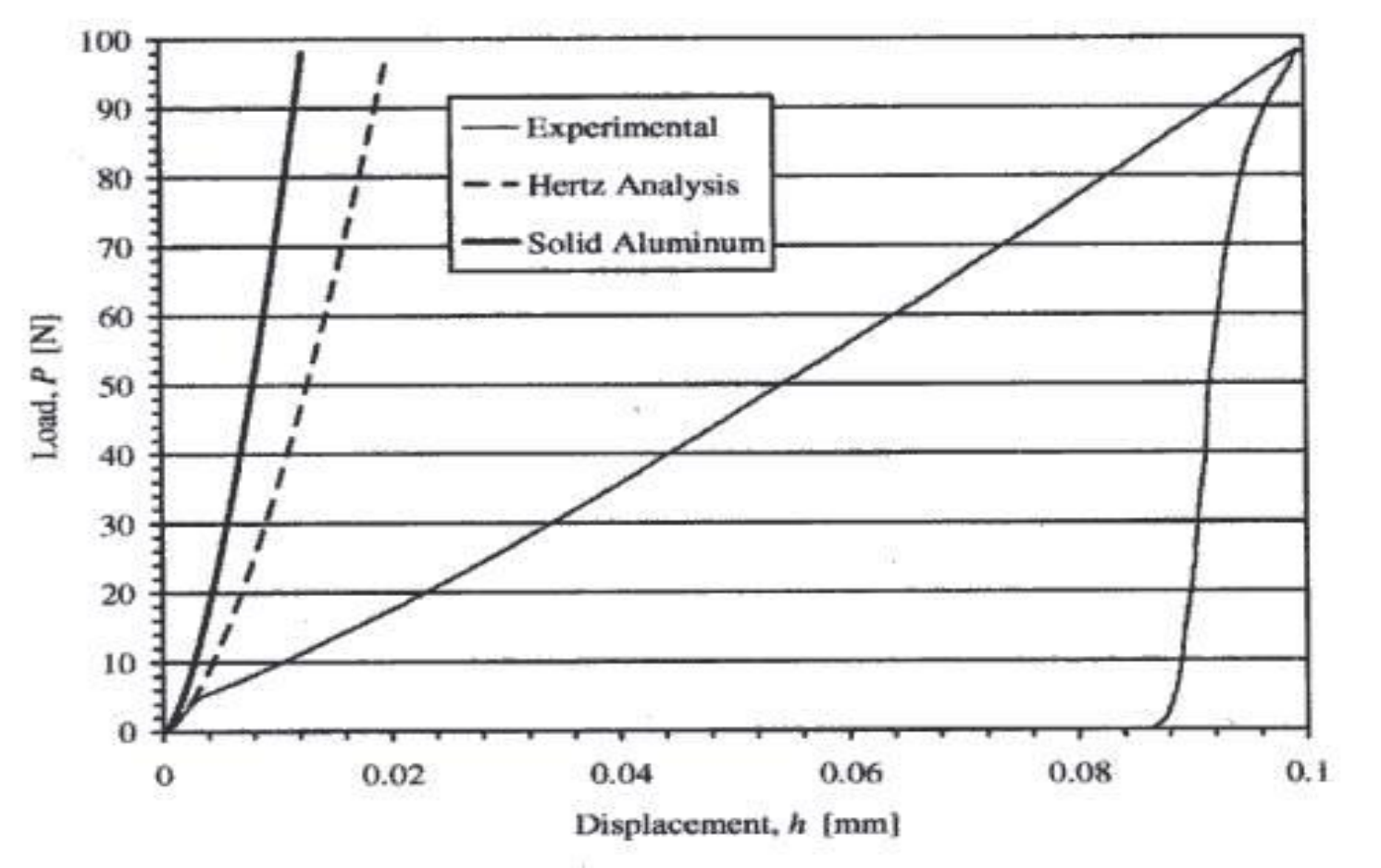

L. Ferranti, Jr., R.W. Armstrong, and N.N. Thadhani, *Mater. Sci. Eng. A*, **371**, 252-255 (2004)

Reversible Hertzian result for an MgO (001) crystal surface

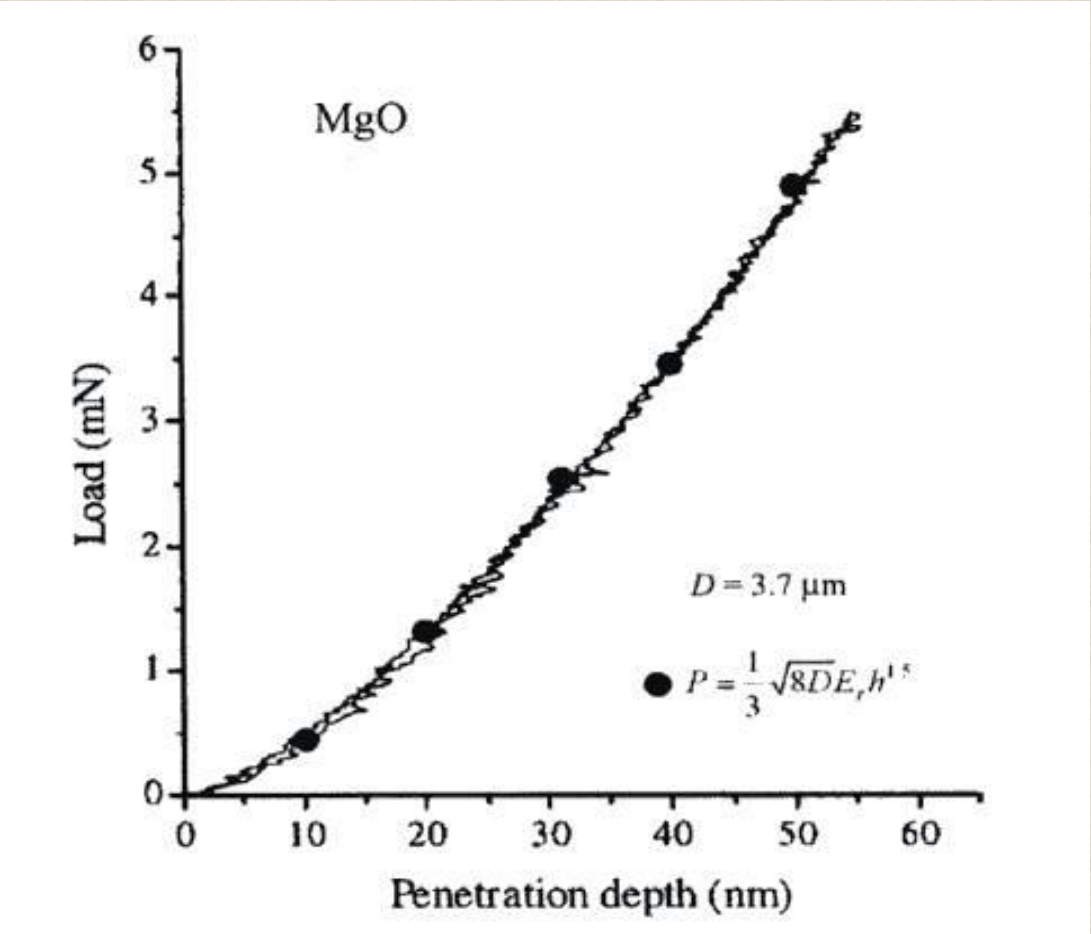

R.W. Armstrong, L. Ferranti, Jr., and N.N. Thadhani, *Intern. J. Refract. Met. Hard Mater.*, **24**, 11–16 (2006); after C. Tromas et al., *J. Mater. Sci.*, **34**, 5337-5342 (1999)

Reversible Hertzian indentation behavior for an indented α-Al_2O_3 (0001) crystal surface

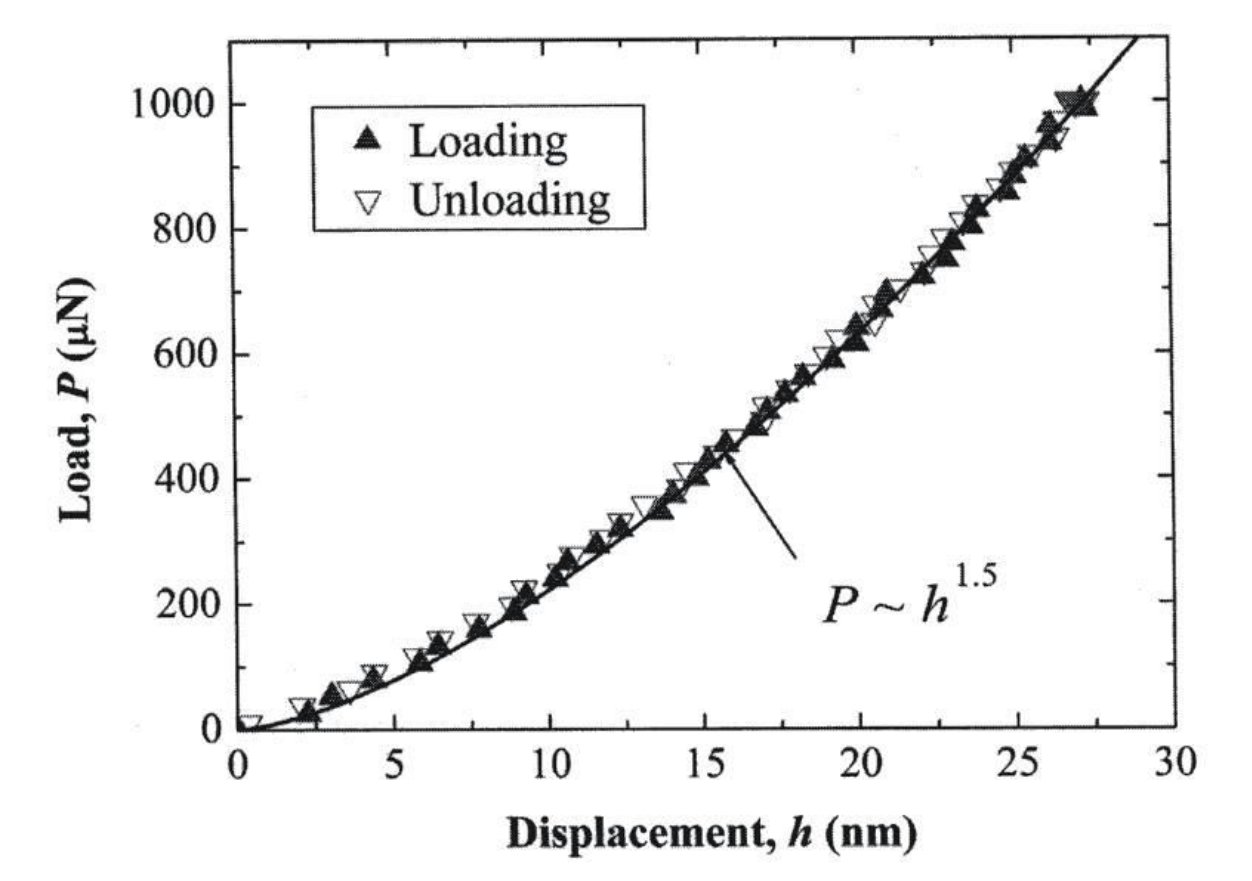

C. Lu, Y.-W. Mai, P.L. Tam and Y.G. Shen, *Philos. Mag. Letts.*, **87** (2007) 409-415.

Elastic/plastic indentation of an MgO (001) crystal surface

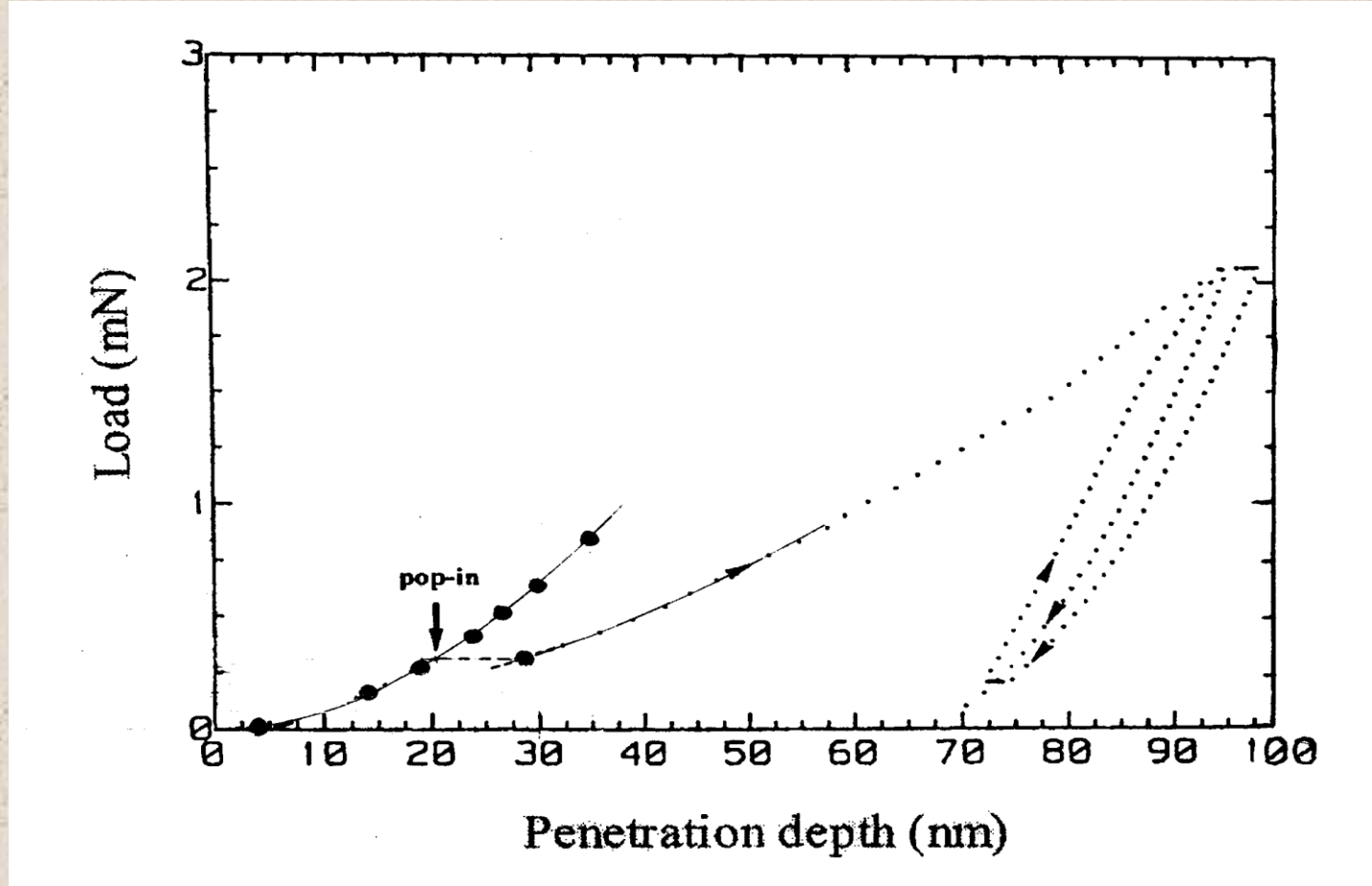

R.W. Armstrong, and W.L. Elban, *Exp. Mech.*, **50** (2010) 545-552; after M.M. Chaudhri, *Philos. Mag. Lett.*, **77** (1998) 7-16

MgO elastic/plastic/cracking comparison

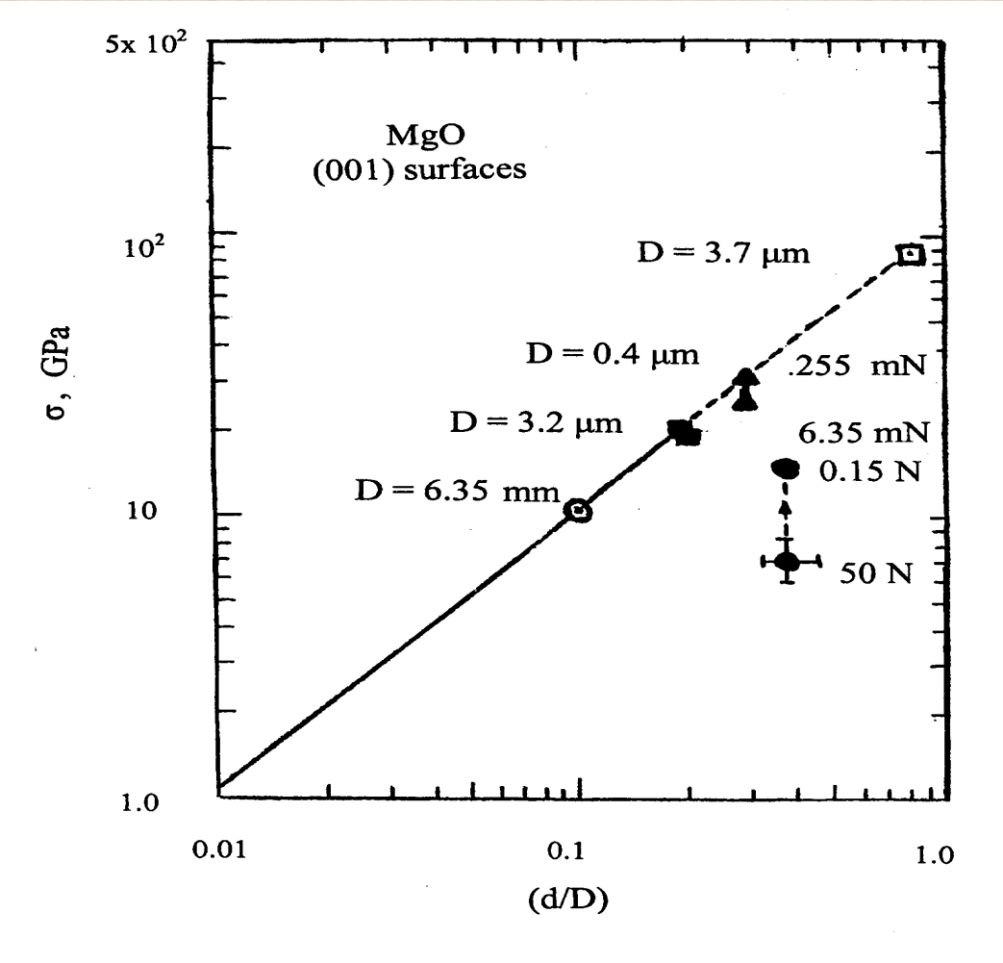

R.W. Armstrong and W.L. Elban, *Exp. Mech.*, **50** (2010) 545-552

Elastic/plastic indentation made with a larger tip diameter (of 3.2 μm as compared with 0.4 μm) applied to another MgO (001) crystal surface

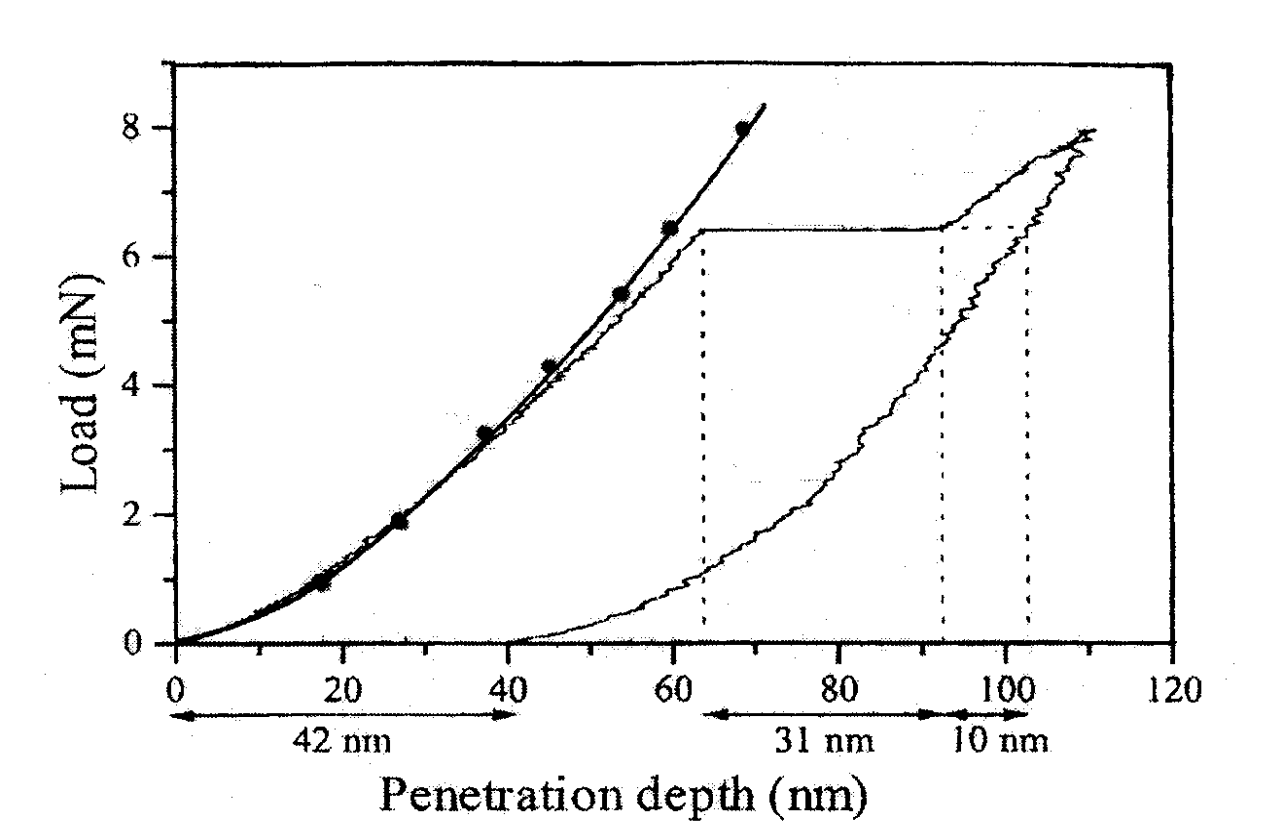

R.W. Armstrong and W.L. Elban, *Exp. Mech.*, **50** (2010) 545-552; after C. Coupeau *et al.*, Dislocations in Solids, edited by F.R. N. Nabarro and J.P. Hirth, **12**, Chap. 67 (Elsevier Ltd., Oxford, 2004) pp. 273-338.

Trough depth measurement at the 31 nm pop-in indentation

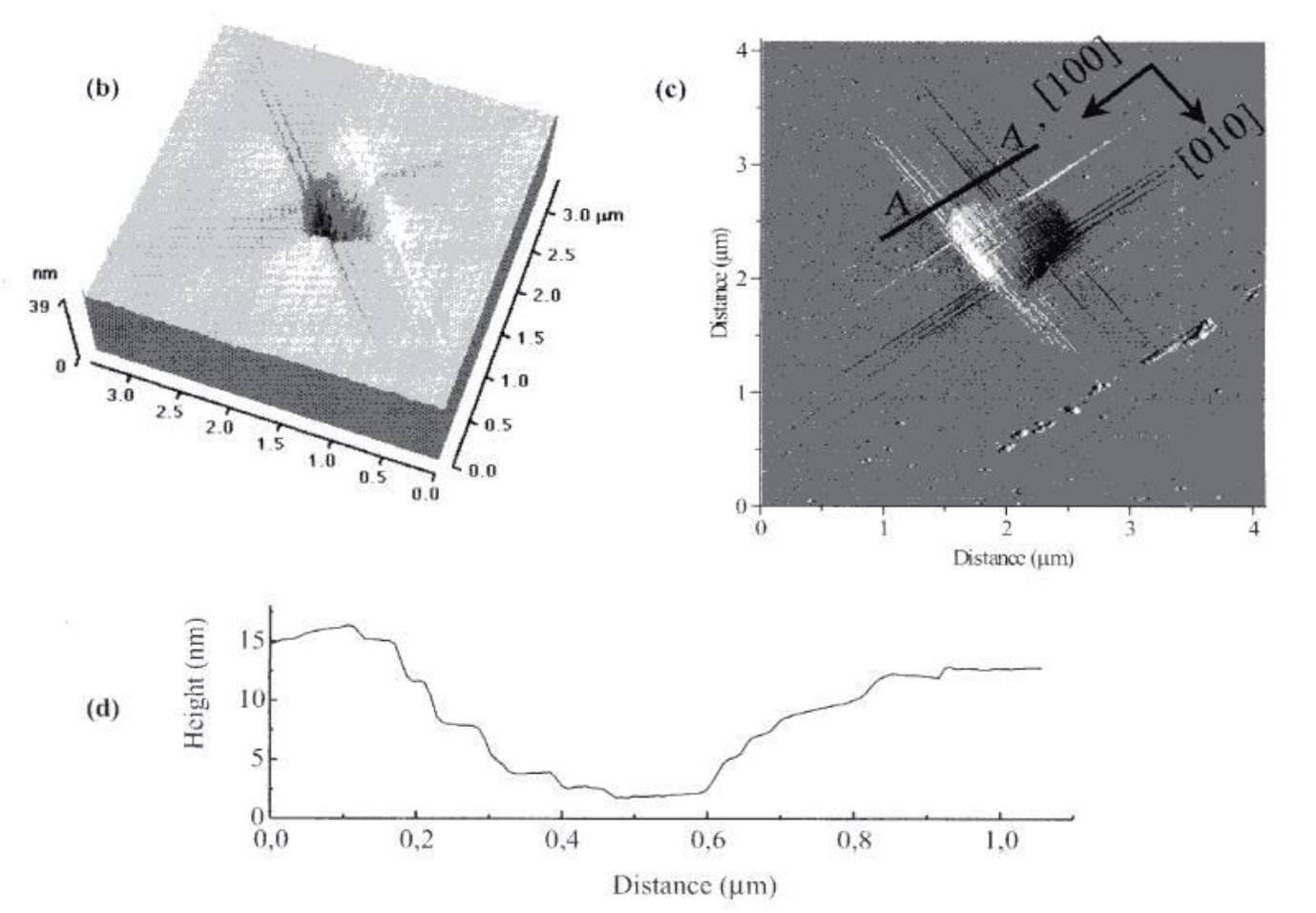

C. Coupeau, J.-C. Girard and J. Rabier, *Dislocations in Solids*, **12**, edited by F.R.N. Nabarro and J.P. Hirth (Elsevier, Ltd., Oxford, 2004) pp. 273-338

Screw dislocation "troughs" at an aligned MgO microindentation

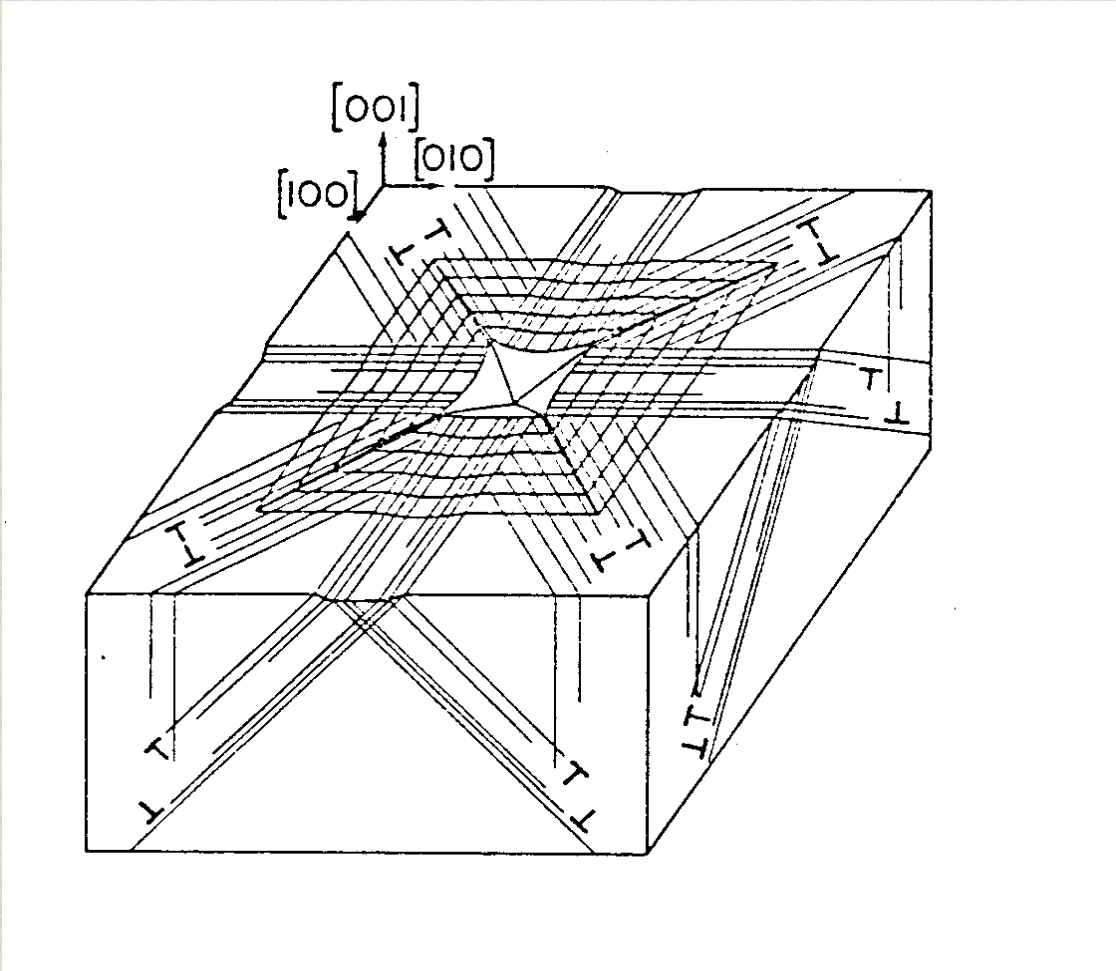

Reported measurement of an ~14 nm trough depth corresponds with an ~31 nm indentation depth; R.W. Armstrong and W.L. Elban, *Exp. Mech.*, **50**, 545-552 (2010)

Smaller elastic vs. “pop-in” displacement for Ni (001) crystal surface

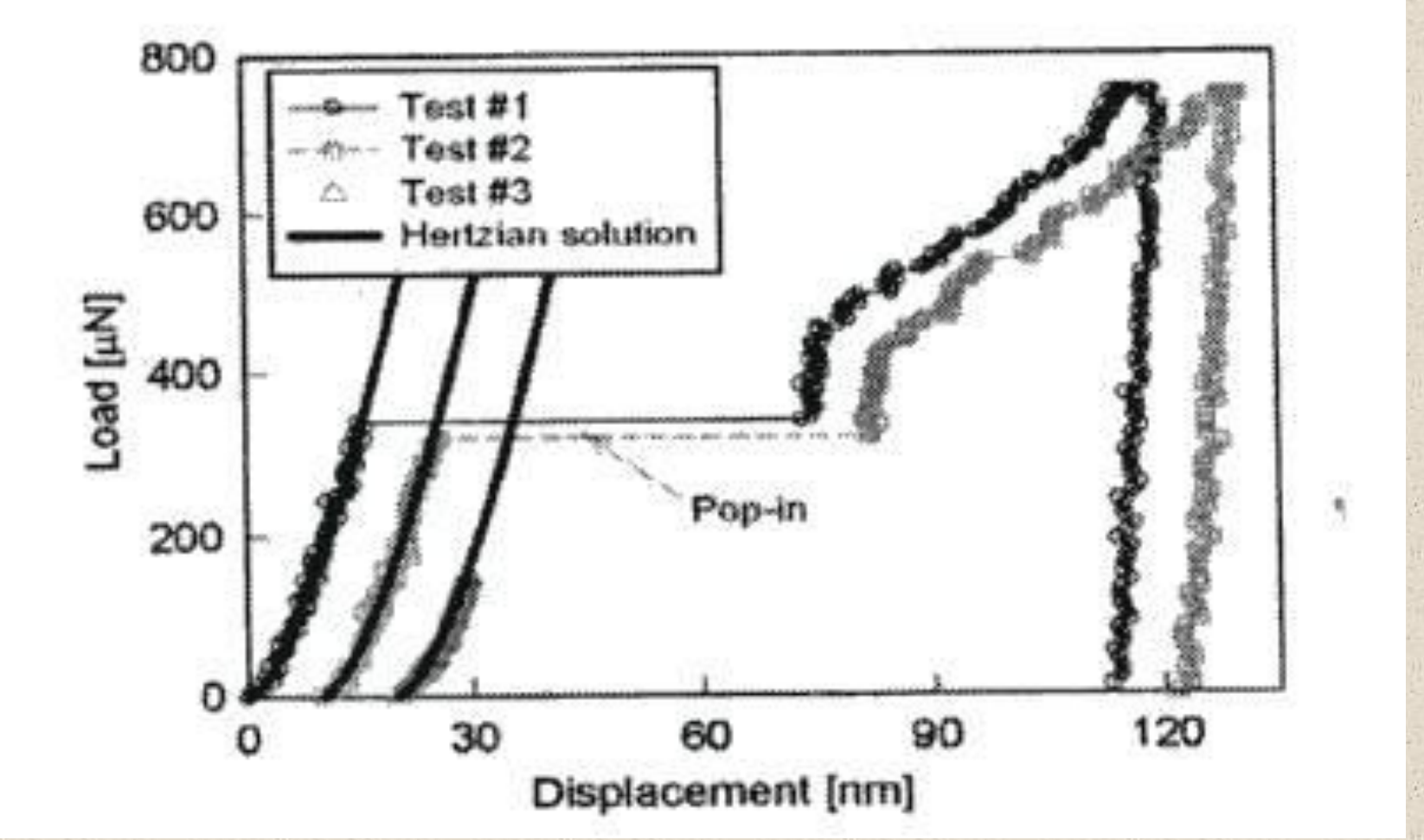

S. Shim, H. Bei, E.P. George and G.M. Pharr, *Scr. Mater.*, **59**, 1095-1098 (2008)

Nano-hardness application to grain boundaries in ultra-low C steel

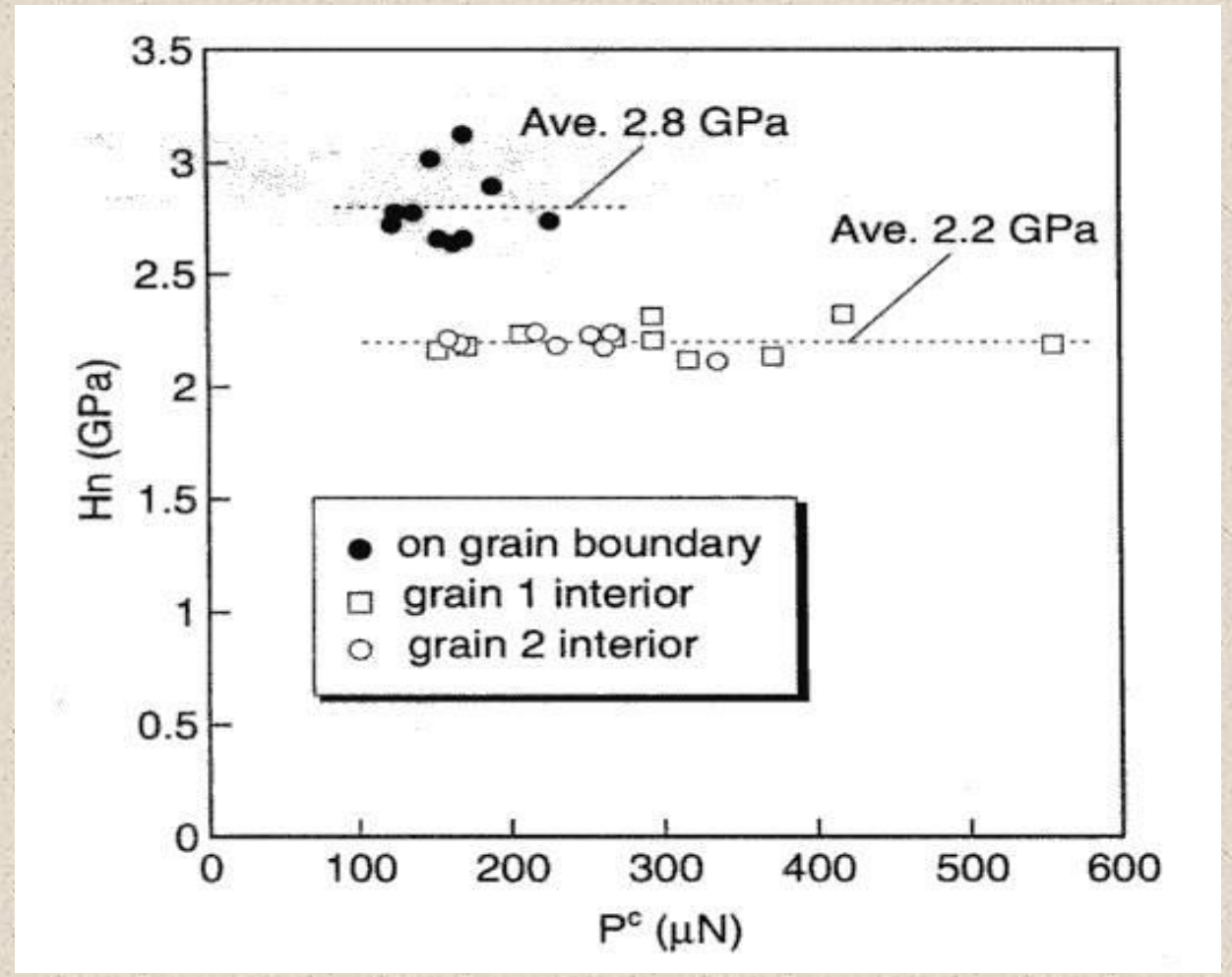

T. Ohmura and K. Tsuzaki, *J. Mater. Sci.*, **42** (2007) 1728-1732.

Grain boundary/volume micro-hardnesses in Nb

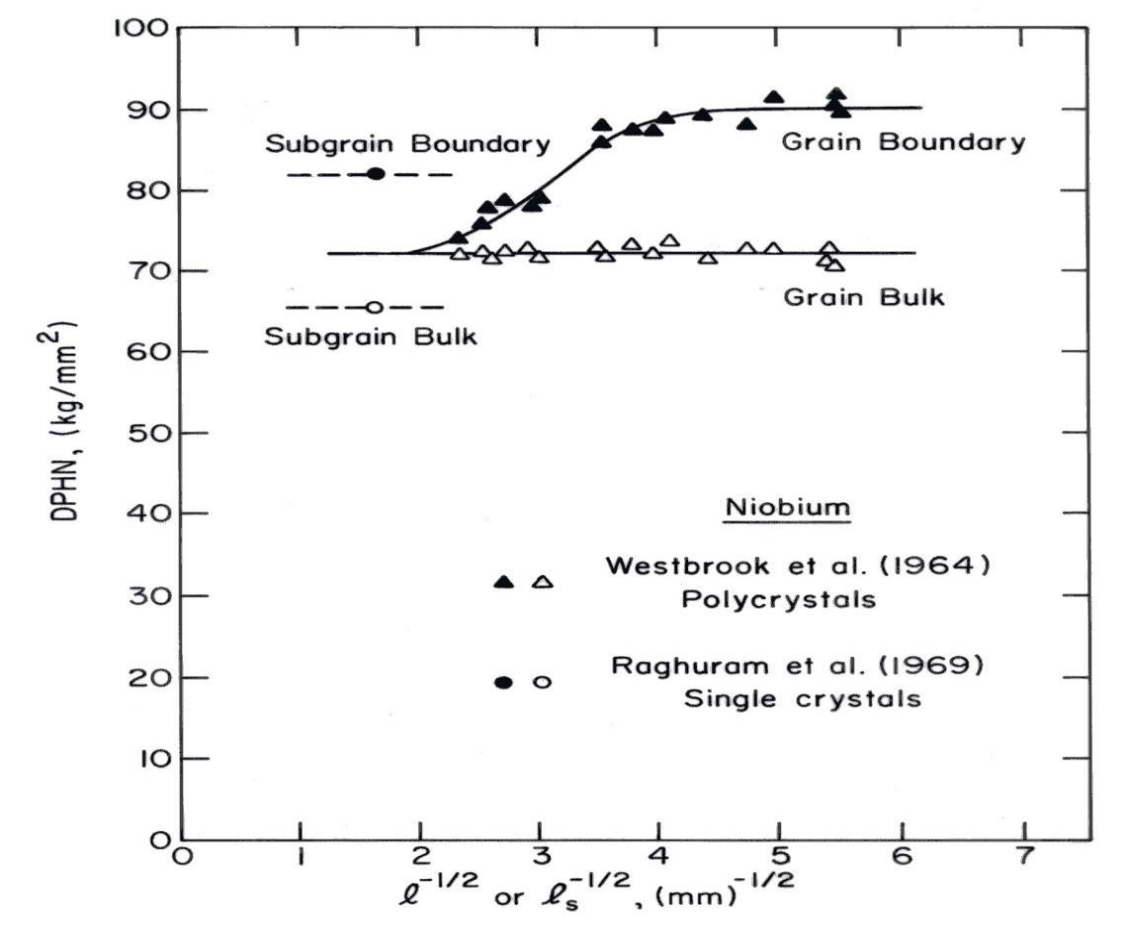

J.H. Westbrook, *Metall. Rev*., **9**. 415ff (1964); A.C. Raghuram, R.W. Armstrong and R.E. Reed, *J. Appl. Phys*., **40**, 4666-4668 (1969)

Hall-Petch hardness dependence on grain size

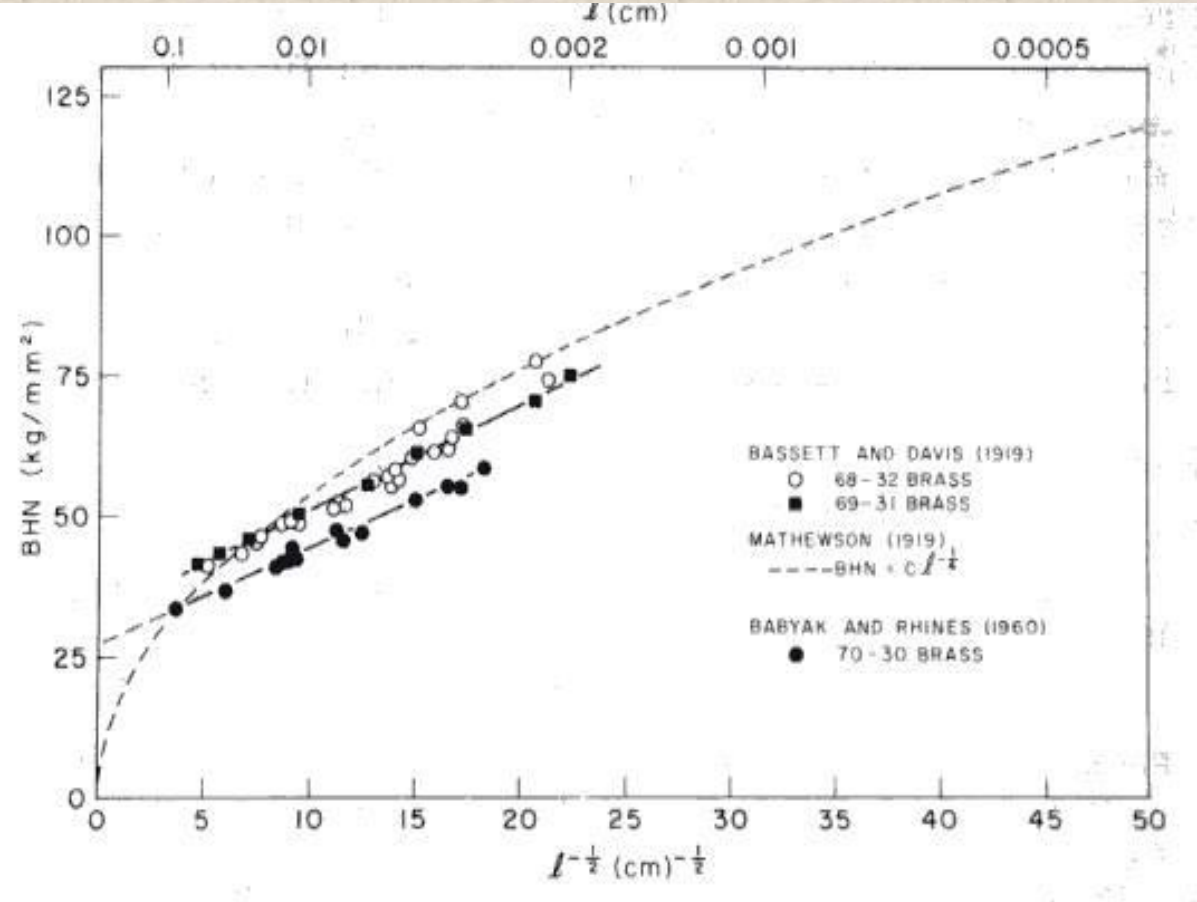

P.C. Jindal and R.W. Armstrong, *Trans. TMS-AIME*, **239** (1967) 1856-1857; after E.O. Hall, *Nature*, **173** (1954) 948-949.

H-P hardness relation for α-Ti

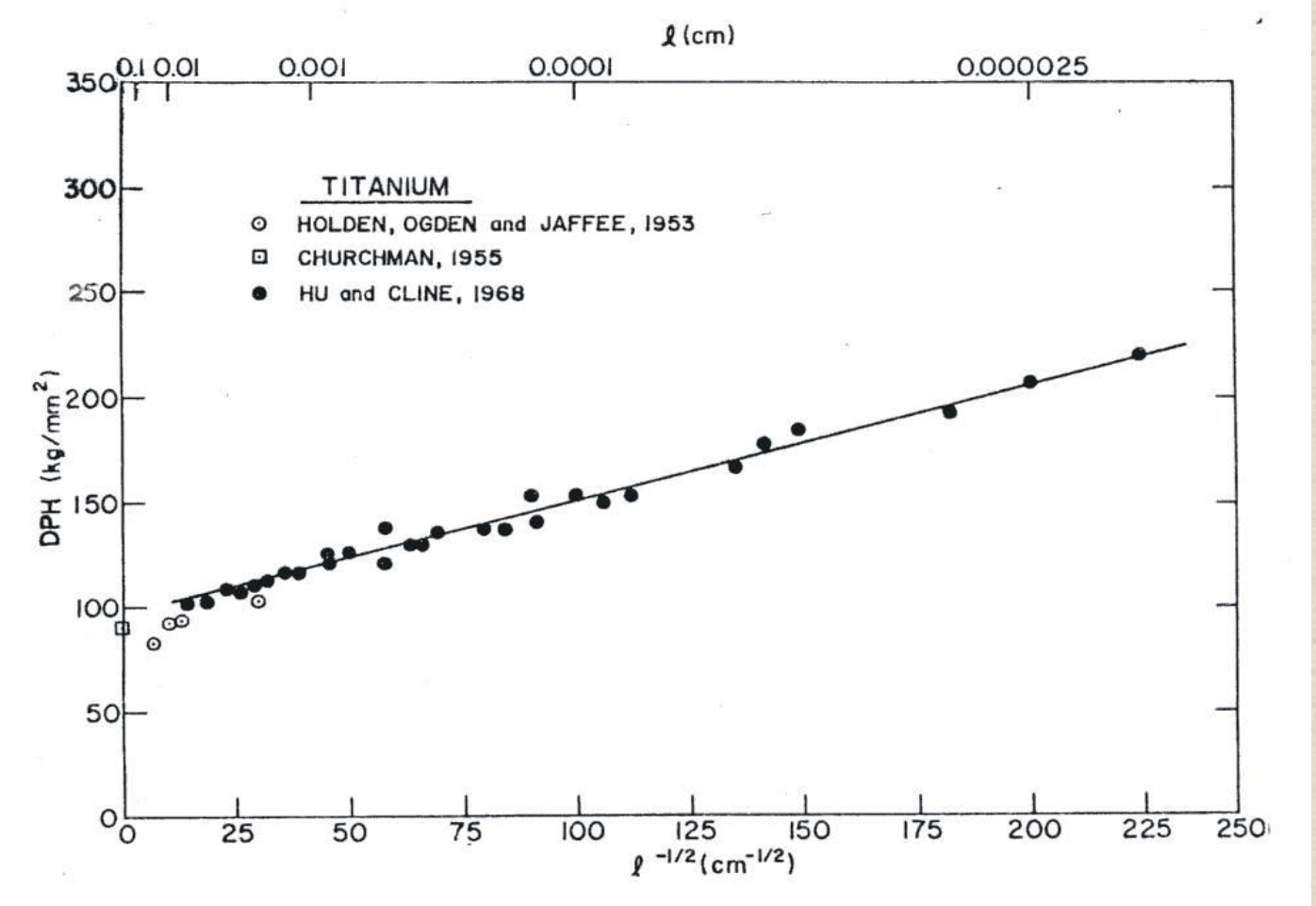

R.W. Armstrong and P.C. Jindal, *Trans. TMS-AIME*, **242**, 2513 (1968)

H-P results for Cr electroplate and bulk material

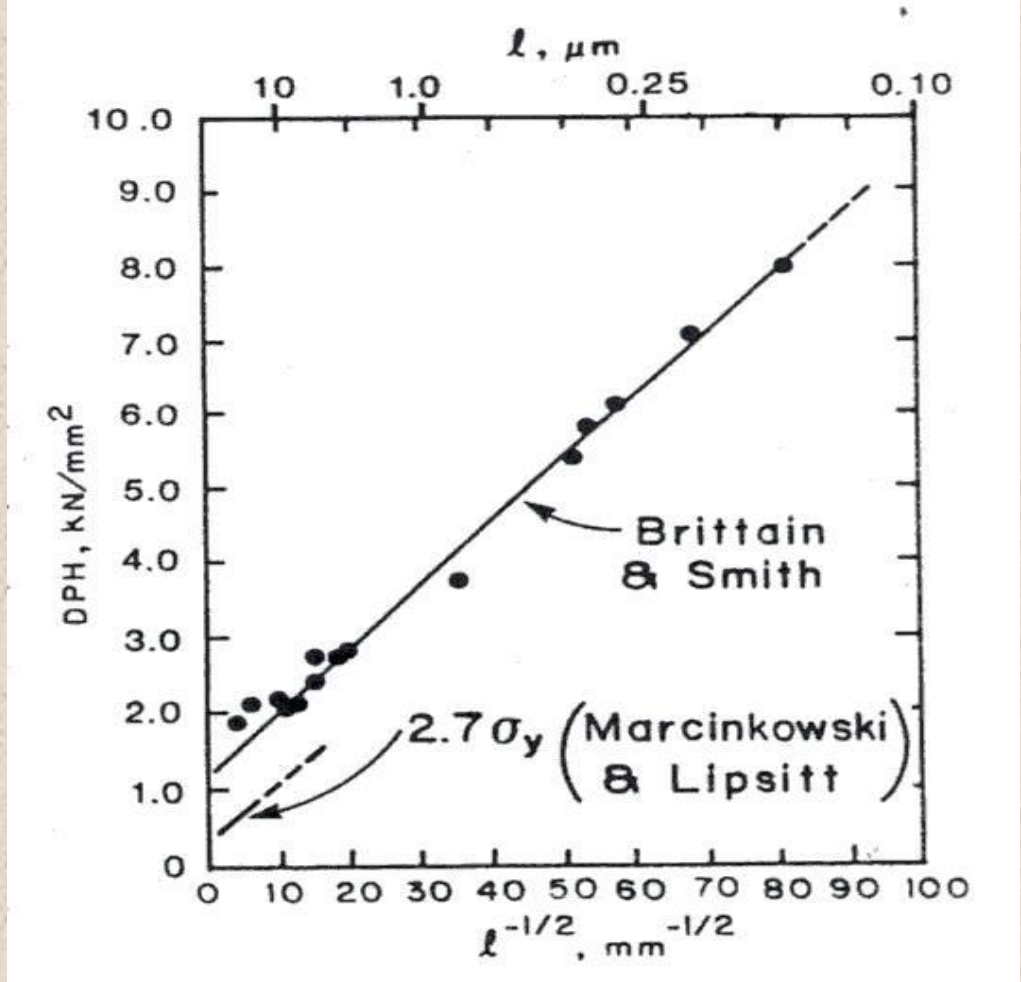

C.P. Brittain, R.W. Armstrong and G.C. Smith, *Scr. Metall.*, **19**, 89-92 (1985)

WC-Co particle/binder size dependent composite hardness, with Hall-Petch values, H_{WC} and H_m, plotted on the ordinate axes

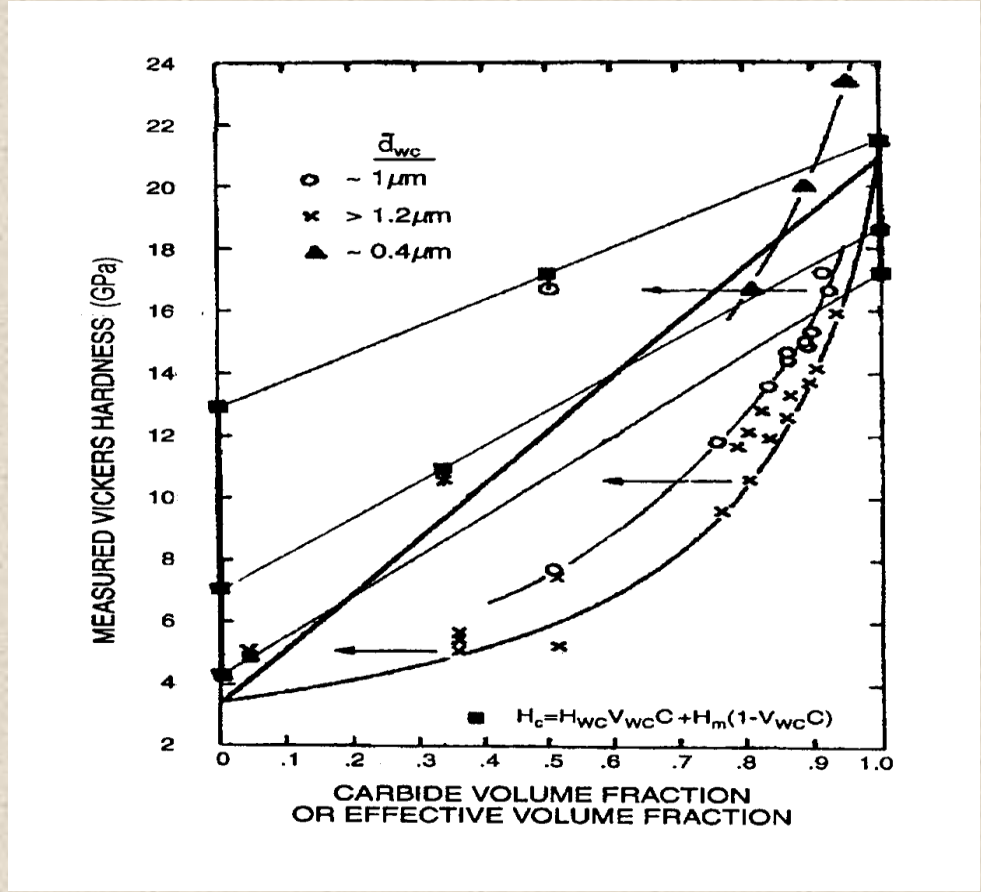

R.W. Armstrong, *Rev. Adv. Mater. Sci.*, **19**, 13-40 (2009); after C.-H. Lee and J. Gurland, *Mater. Sci. Eng.*, **33**, 125-133 (!978).

X-ray topograph of a macro-indentation in MgO

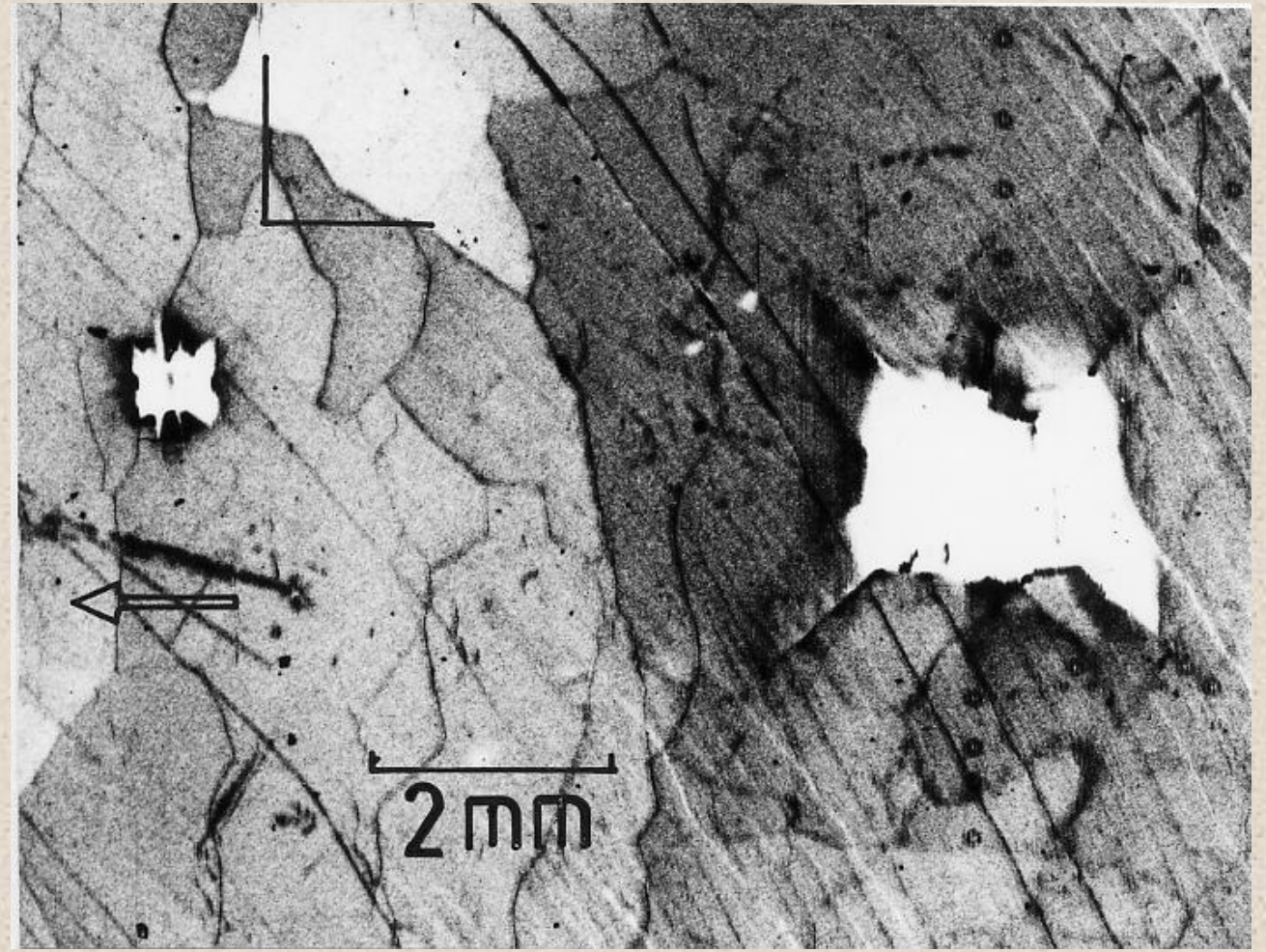

K.-C. Yoo, R.G. Rosemeier, W.L. Elban and R.W. Armstrong, *J. Mater. Sci. Lett.*, **3**, 560-562 (1984)

Indentation fracture mechanics measurements for MgO

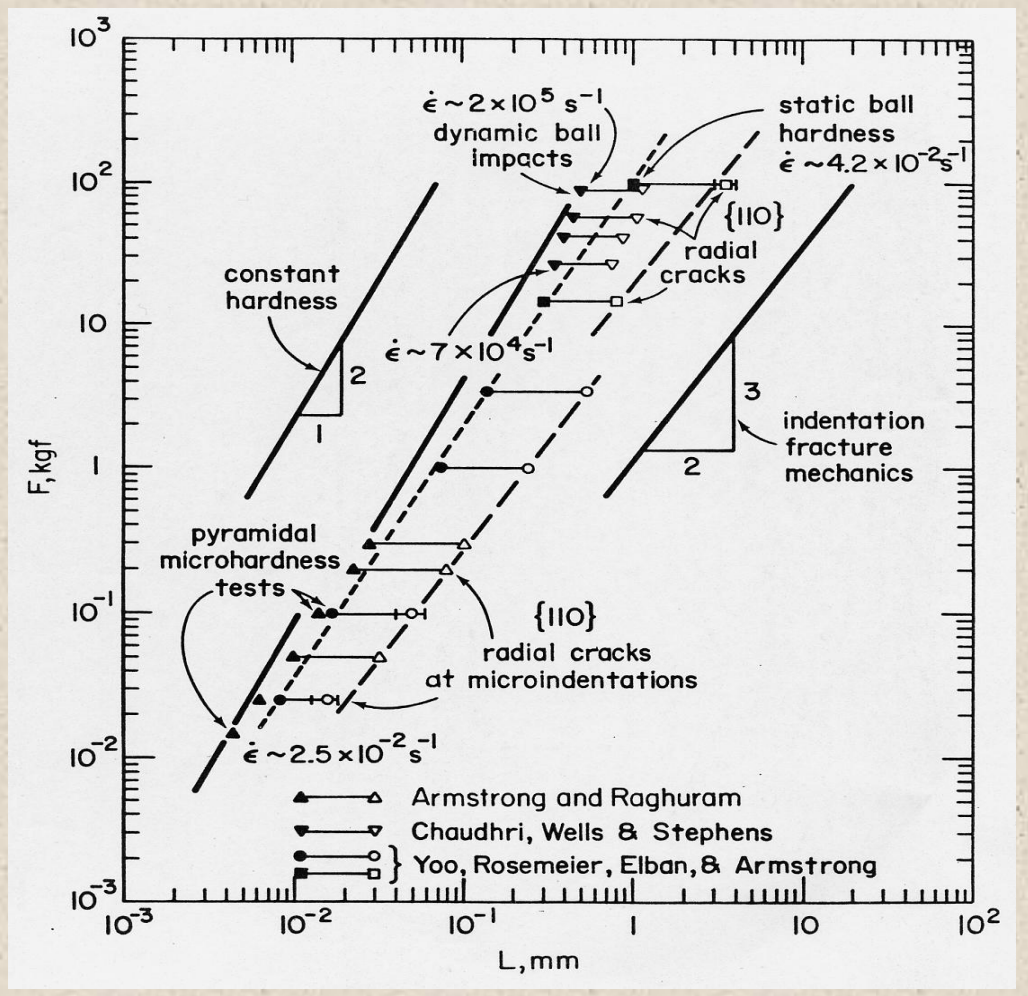

K.-C. Yoo, R.G. Rosemeier, W.L. Elban, and R.W. Armstrong, *J. Mater. Sci. Lett.*, **3**, 560-562 (1984)

Indentation fracture mechanics comparison of MgO and RDX

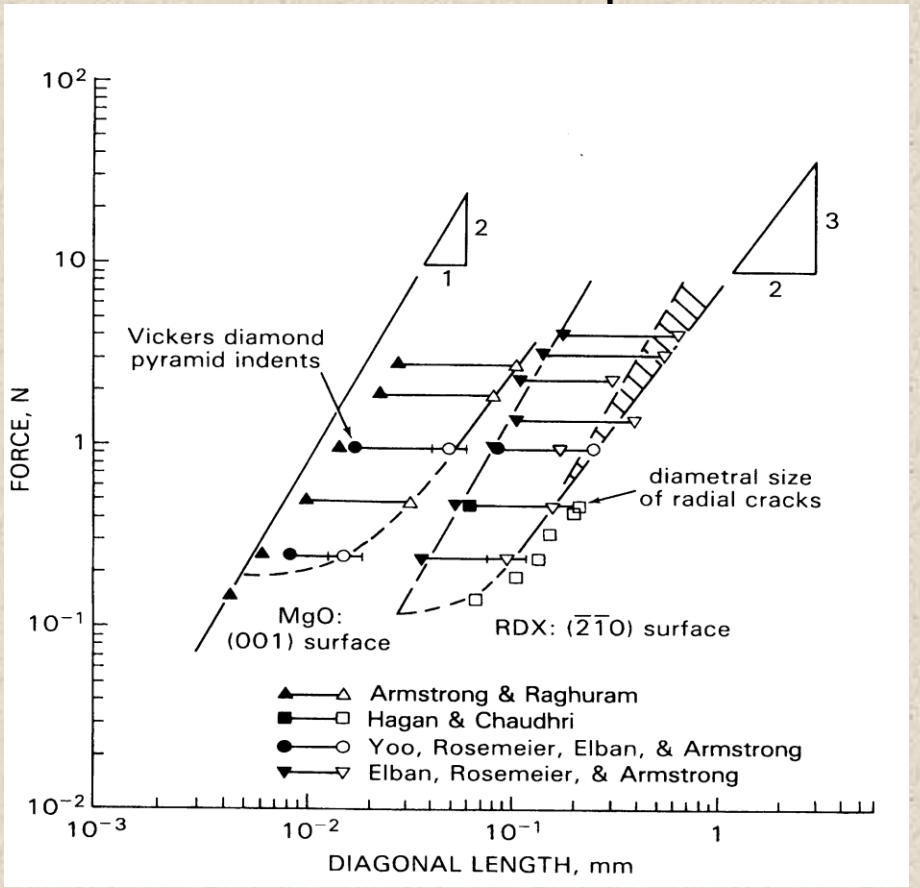

$$K_{Ic} = \chi(\Delta P/\Delta[c^{3/2}])$$

R.W. Armstrong and W.L.Elban, *Mater. Sci. Eng. A*, **111**, 35-43 (1989); after J.T. Hagan and M.M. Chaudhri, *J. Mater. Sci.*, **12**, 1055-1058 (1977)

Elastic, plastic, cracking behavior of Si crystals

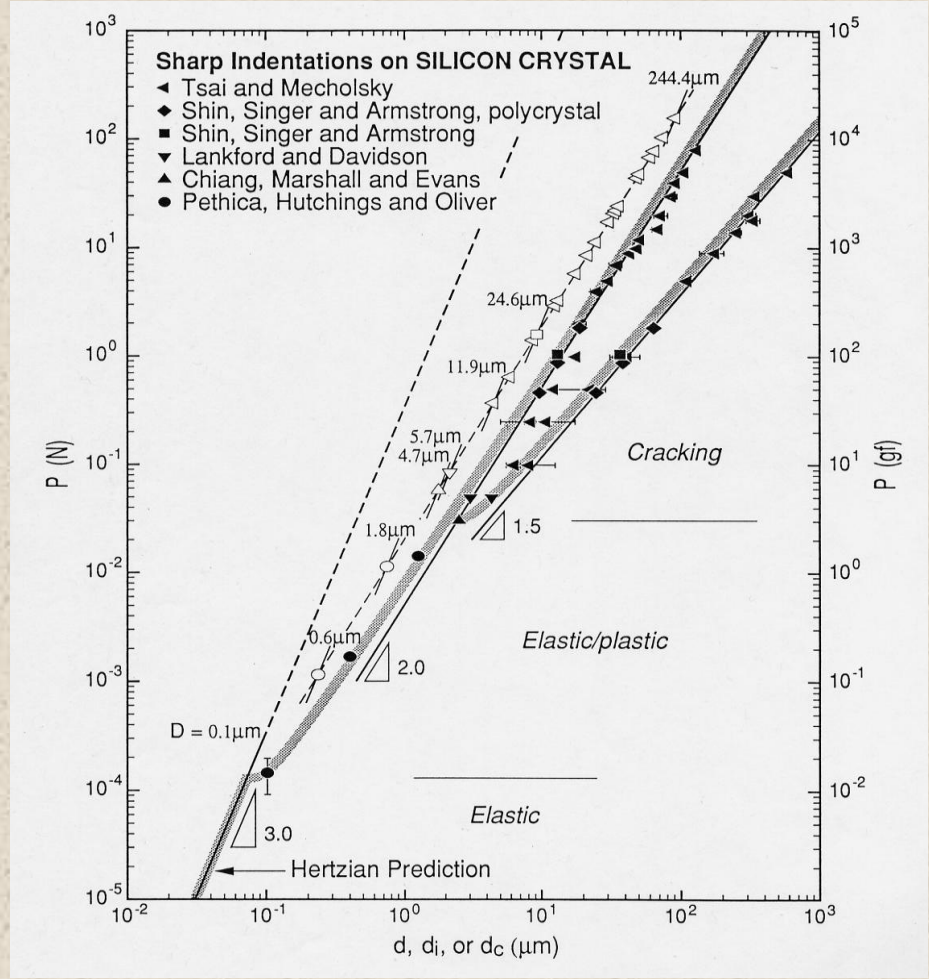

R.W. Armstrong, J.J. Mecholsky, H. Shin and Y.L. Tsai, *J. Mater. Sci. Lett.* **12**, 1274-1275 (1993)

Ball indentation tests on silicon crystals

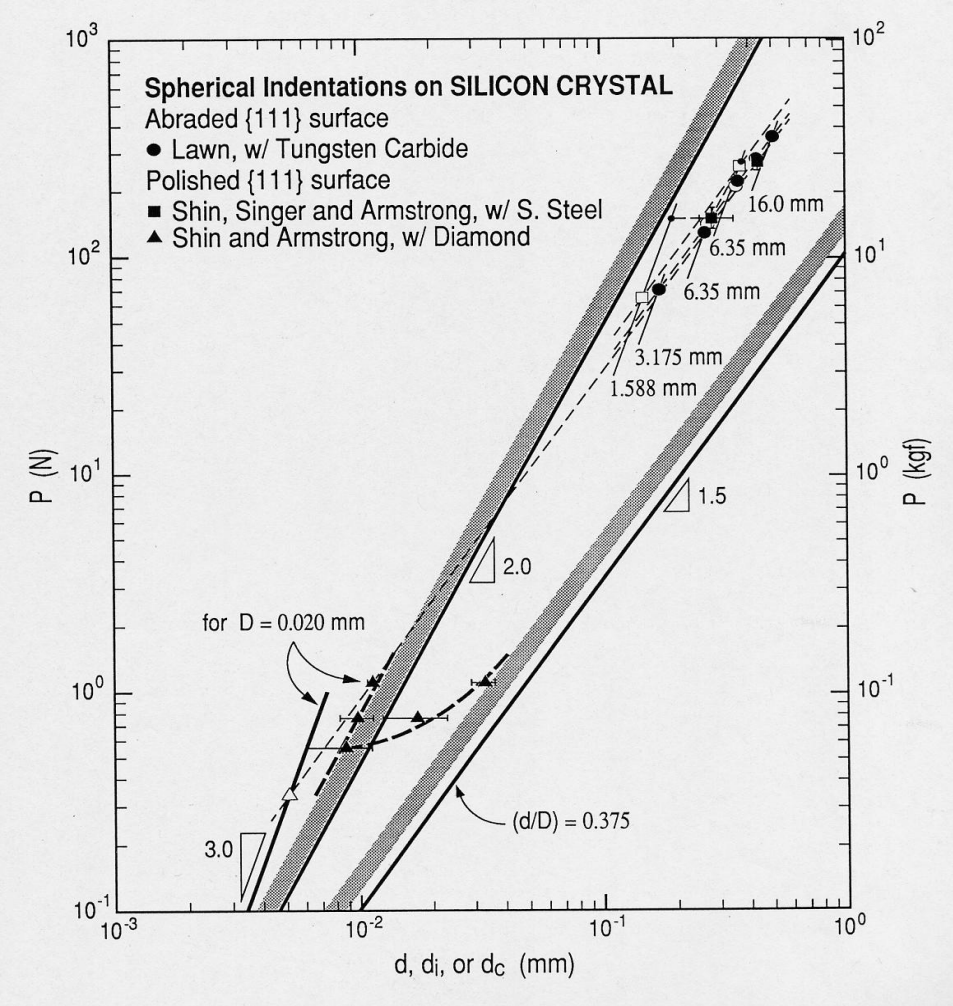

R.W. Armstrong, A.W. Ruff and H. Shin, *Mater. Sci. Eng. A*, **209**, 91-96 (1996).

H-P type K_{Ic} dependence on grain size for Al_2O_3

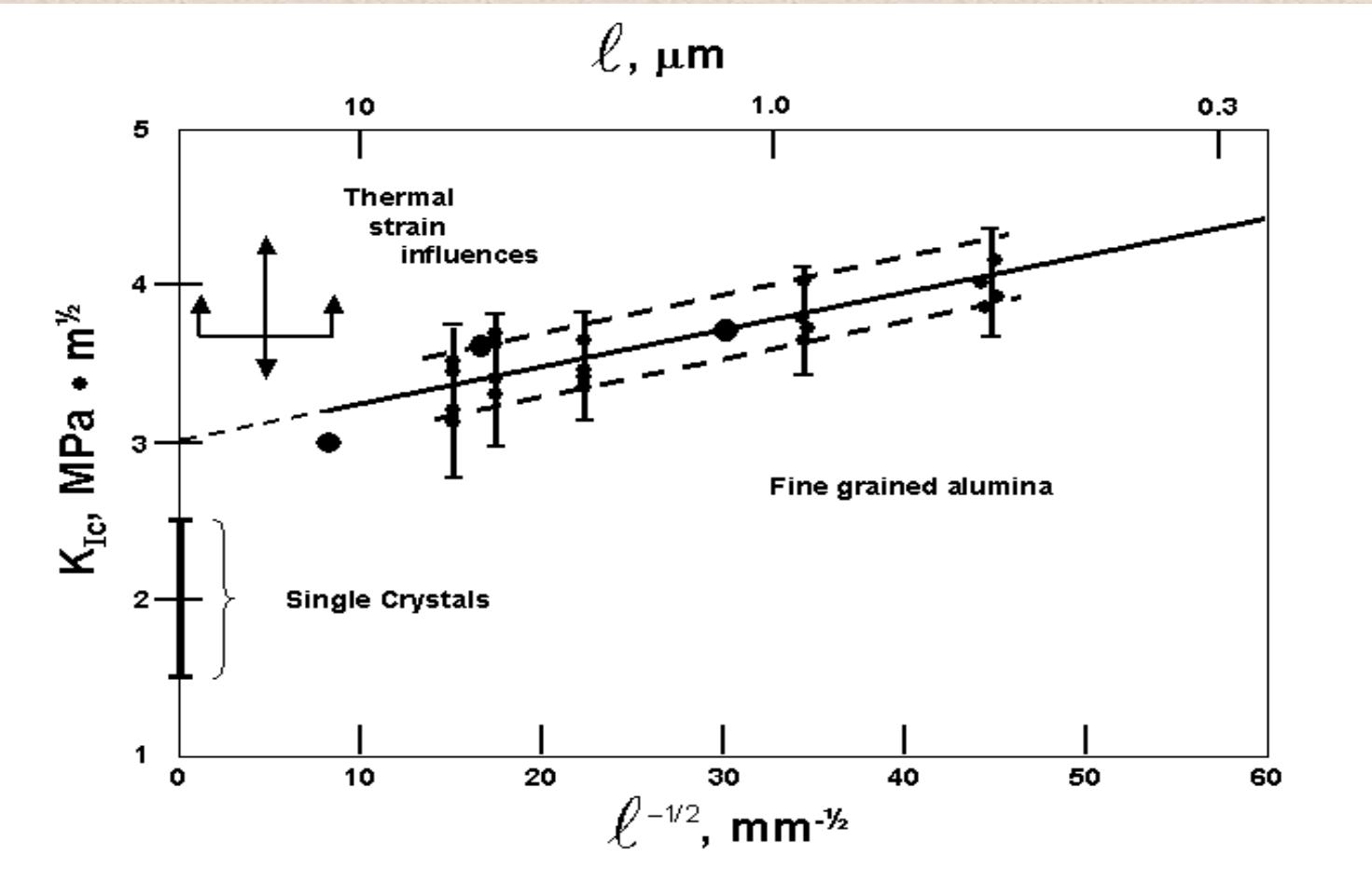

R.W. Armstrong, *Intern. J. Refract. Met. & Hard Mater.*, **19**, 251-255 (2001); after experimental results of Rice (1997), Franco, Roberts and Warren (1997), and Muchtar and Lim (1998).

Comparison of grain, crack, and plastic zone dimensions for Al_2O_3

Table 1. Modeled BCS-based pre-crack fracture stresses

ℓ, mm	K_{Ic}, MPa $m^{1/2}$	c, mm	σ_{F0}, MPa	s, mm	σ_{Fc}, MPa
0.0012	3.16	0.0213	536	0.01365*	335**
0.0038	3.09	0.0225	461	0.01764	305.5
0.01984	2.95	0.0245	415	0.01984	277.6
0.0012	2.93	0.3301	536	0.01735*	110.5^
0.0038	3.06	0.3239	461	0.01730	95.9
0.01984	3.23	0.3146	415	0.02379	102.75

$$*s = (\pi/8)(K_{Ic}/\sigma_{F0})^2$$

$$**\sigma_{Fc} = \sigma_{F0}\sqrt{([s/c]/\{1+[s/c]\})}$$

$$^\sigma_{Fc} = (\sqrt{8}/\pi)\sigma_{F0}\sqrt{(s/c)}$$

R.W. Armstrong and O. Cazacu, *Intern. J. Refract. Met. & Hard Mater.*, **24**, 129-134 (2006)

$K_{Ic} = A_0[\sigma_{0C} + k_C \ell^{-1/2}]s^{1/2}$ and with s proportional to $\ell \sim \lambda$

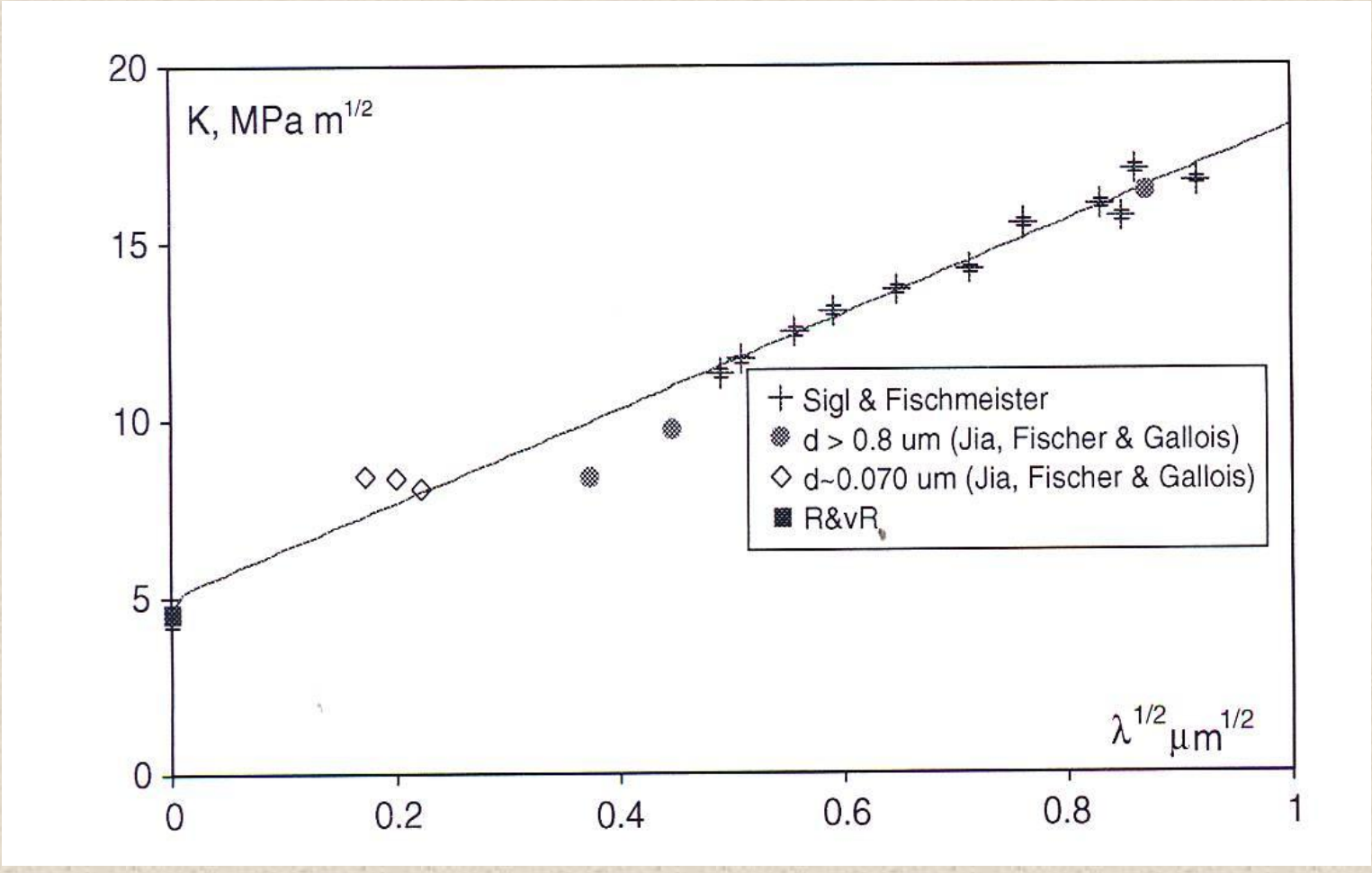

R.W. Armstrong and O. Cazacu, *Intern. J. Refract. Met. & Hard Mater.*, **24**, 129-134 (2006).

SUMMARY

1. Macro-, micro- and nano-indentation hardness results are presented for certain aspects of the elastic, plastic, and cracking indentation behaviors of crystal, polycrystal and polyphase composite materials.
2. Elastic modulus measurements, obtained with difficulty in macro-indentation tests, are a natural byproduct of nano-indentation measurements.
3. Crystal hardness testing can be usefully employed to demonstrate the role of dislocation pile-ups in producing cracks.
4. Whereas nano- and micro-indentations can be employed to differentiate between grain boundary and grain volume hardnesses, micro- or macro-indentation testing over multiple grains can be usefully employed to determine Hall-Petch type reciprocal square root of grain size dependencies.
5. Cracking measurements at indentations are shown to be usefully applied to determining indentation fracture mechanics parameters consistent with conventional fracture mechanics measurements.